NeuroImage 44 (2009) 1247–1258

Contents lists available at ScienceDirect

NeuroImage

journal homepage: www.elsevier.com/locate/ynimg

# Regional white matter volume differences in nondemented aging and Alzheimer's disease

David H. Salat [a,b,*], Douglas N. Greve [a,b], Jennifer L. Pacheco [a,b], Brian T. Quinn [a,b], Karl G. Helmer [a,b], Randy L. Buckner [a,b,c,d], Bruce Fischl [a,b,e]

[a] Department of Radiology, Massachusetts General Hospital, Boston MA, USA
[b] MGH/MIT/HMS Athinoula A. Martinos Center for Biomedical Imaging, Charlestown MA, USA
[c] Department of Psychology, Center for Brain Science, Harvard University, Cambridge MA , USA
[d] Howard Hughes Medical Institute, USA
[e] MIT Computer Science and Artificial Intelligence Laboratory, Cambridge MA, USA

ARTICLE INFO

*Article history:*
Received 2 May 2008
Revised 15 October 2008
Accepted 16 October 2008
Available online 5 November 2008

ABSTRACT

Accumulating evidence suggests that altered cerebral white matter (WM) influences normal aging, and further that WM degeneration may modulate the clinical expression of Alzheimer's disease (AD). Here we conducted a study of differences in WM volume across the adult age span and in AD employing a newly developed, automated method for regional parcellation of the subcortical WM that uses curvature landmarks and gray matter (GM)/WM surface boundary information. This procedure measures the volume of gyral WM, utilizing a distance constraint to limit the measurements from extending into the centrum semiovale. Regional estimates were first established to be reliable across two scan sessions in 20 young healthy individuals. Next, the method was applied to a large clinically-characterized sample of 299 individuals including 73 normal older adults and 91 age-matched participants with very mild to mild AD. The majority of measured regions showed a decline in volume with increasing age, with strong effects found in bilateral fusiform, lateral orbitofrontal, superior frontal, medial orbital frontal, inferior temporal, and middle temporal WM. The association between WM volume and age was quadratic in many regions suggesting that WM volume loss accelerates in advanced aging. A number of WM regions were further reduced in AD with parahippocampal, entorhinal, inferior parietal and rostral middle frontal WM showing the strongest AD-associated reductions. There were minimal sex effects after correction for intracranial volume, and there were associations between ventricular volume and regional WM volumes in the older adults and AD that were not apparent in the younger adults. Certain results, such as the loss of WM in the fusiform region with aging, were unexpected and provide novel insight into patterns of age associated neural and cognitive decline. Overall, these results demonstrate the utility of automated regional WM measures in revealing the distinct patterns of age and AD associated volume loss that may contribute to cognitive decline.

Published by Elsevier Inc.

## Introduction

Accumulating evidence suggests that processes associated with nondemented aging as well as the degenerative processes of Alzheimer's disease (AD) have a negative effect on cerebral white matter (WM). The regional predilection for WM degeneration and the contribution of this tissue loss to cognitive and neural dysfunction is of considerable interest, but has been difficult to quantify. The anatomic organization of brain WM is highly complex and not visible on a standard T1 weighted MRI scan. However, WM proximal to a cortical region preferentially contains afferent and efferent fibers associated with that cortical region, and thus, the condition of this adjacent tissue provides information about the integrity of specific neural systems. In the present paper we apply a novel, automated method to explore local WM integrity in normal aging and AD.

Quantification of age and AD associated alterations in WM volume has been a goal in postmortem (Anderson et al., 1983; Hubbard and Anderson, 1981; Meier-Ruge et al., 1992; Miller et al., 1980) as well as early imaging studies using CT (de Leon et al., 1989; Gado et al., 1983; Obara et al., 1994). MRI studies have examined whole brain WM volume, volume of selective WM regions, and abnormal WM signal (Christiansen et al., 1994; de Leeuw et al., 2001; DeCarli et al., 1996; DeCarli et al., 1995; Head et al., 2005; Jernigan et al., 1991a; Jernigan et al., 1991b; Mungas et al., 2005; Mungas et al., 2002; Pfefferbaum et al., 1994; Raz et al., 1997; Rusinek et al., 1991; Salat et al., 1999; Sullivan

* Corresponding author. MGH/MIT/HMS Athinoula A. Martinos Center for Biomedical Imaging, MGH Department of Radiology, Building 149, 13th St., Mail Code 149 (2301), Charlestown, MA, USA. Fax: +1 617 726 7422.
*E-mail address:* salat@nmr.mgh.harvard.edu (D.H. Salat).

1053-8119/$ – see front matter. Published by Elsevier Inc.
doi:10.1016/j.neuroimage.2008.10.030

et al., 1995; Udaka et al., 2002; Wahlund et al., 1994). The majority of these studies generally demonstrate that there is a significant loss of WM volume and an increase in abnormal WM signal with aging (Guttmann et al., 1998; Jernigan et al., 1991a; Raz et al., 1997; Resnick et al., 2000), however, several studies utilizing differing procedures have also demonstrated relatively little change in WM volume in aging and associated disease (Double et al., 1996; Jernigan et al., 1991a; Jernigan et al., 1991b; Obara et al., 1994; Rusinek et al., 1991; Sullivan et al., 1995; Tanabe et al., 1997). These disparate findings could be due to the fact that WM volume loss may have a highly specific temporal and spatial pattern. For example, WM volume is reported to be relatively stable until approximately the fifth decade of life in healthy adults (Bartzokis et al., 2001; Pfefferbaum et al., 1994). Controversially, WM changes are reported to contribute in a complex manner (Burns et al., 2005; DeCarli et al., 1995; Fotenos et al., 2005; Hirono et al., 2000a; Hirono et al., 2000b; Smith et al., 2000; Stout et al., 1996; Tanabe et al., 1997; Tohgi et al., 1998; Waldemar et al., 1994) or not at all (Rusinek et al., 1991; Wahlund et al., 1994) to the clinical expression of AD. For example, Smith et al. reported an association between normal WM volume and dementia which was not true for periventricular hyperintensities (Smith et al., 2000). Other studies have demonstrated a significant role for WM signal abnormalities in AD dementia but are consistent with a modulatory effect of symptoms rather than a direct contribution to AD (Burns et al., 2005). Wu et al. (2002), based on analysis of two MR and PET studies, concluded that changes associated with AD and commonly observed WM changes linked to vascular disease are synergistic contributors to dementia (Wu et al., 2002).

More recently developed imaging techniques, such as diffusion imaging, magnetization transfer imaging, spectroscopy, and other advanced MR procedures have contributed additional information about the vulnerability of WM to degenerative processes (Armstrong et al., 2004; Bartzokis et al., 2003; Choi et al., 2005; Head et al., 2004; Madden et al., 2004; Pfefferbaum and Sullivan, 2003; Pfefferbaum et al., 2000; Rose et al., 2000; Rose et al., 2006; Salat et al., 2005a,b; Sandson et al., 1999; Sullivan et al., 2001) and complement studies utilizing histological analysis to understand pathologic mechanisms of WM degeneration (Braak and Braak, 1989; Hashimoto et al., 2003; Hyman et al., 1984; Kovari et al., 2007; Roher et al., 2002; Thal et al., 1998; van de Nes et al., 2002; Webster et al., 2006; Xuereb et al., 2000; Yang et al., 2005; Zhukareva et al., 2002). These studies support the important role of WM deterioration in brain aging and dementia, with some specificity to the regional patterns of changes in WM integrity. For example, DTI studies have clarified an anterior to posterior gradient of age effects on brain WM microstructure (Head et al., 2004; Pfefferbaum et al., 2005; Salat et al., 2005a) and altered diffusion measures in temporal or temporal stem WM with AD, with additional effects reported in frontal, parietal, and callosal regions (Bozzali et al., 2002; Hanyu et al., 1998; Head et al., 2004; Kantarci et al., 2001; Salat et al., 2008).

Volumetric studies of WM have been mostly limited in measuring the entire cerebral WM at a coarse spatial scale; regional variation in morphometry has been less accessible. Relatively few studies have examined alterations in WM volume on a regional or lobar basis but notable exceptions exist (Bartzokis et al., 2001; Bigler et al., 2002; Raz et al., 1997; Salat et al., 1999). These studies have demonstrated regional variation in WM volume loss underscoring the importance of more selective regional volumetric measures. Similarly, voxel based morphometry studies reinforce the fact that WM changes regionally accelerated in particular areas including frontal WM and anterior callosum in normal aging (Brickman et al., 2007; Good et al., 2001) and parahippocampal and temporal in preclinical or clinically diagnosed AD (Li et al., 2008; Stoub et al., 2006). However, there is still relatively limited information on the temporal and regional basis of WM volume loss in these conditions. Thus, a procedure to divide cerebral WM into homologous volumetric regions across individuals on T1 images, which are widely available in MR studies including retrospective studies, would be of high value for addressing questions about age and dementia associated WM degeneration.

The current study utilized detailed morphometric procedures to obtain regional WM volume measurements to determine whether WM degeneration is a global or regionally selective process, and the pattern of that degeneration across the adult age span. We employed a newly developed method for automated parcellation of brain WM using morphometric landmarks and GM/WM boundary surface information. This procedure builds on our prior described and validated cortical parcellation technique (Desikan et al., 2006; Fischl et al., 2004), and extends this labeling to the subcortical WM directly underlying the cortical parcellation. We first applied this novel procedure to a sample of individuals that were imaged on two different occasions within a short time period to examine the test–retest reliability of the regional measurements. We next utilized the technique to examine regional volumetric differences in a large sample of healthy younger (YNG) and nondemented older (OLD) adults, and a group of individuals with AD. These initial descriptive results demonstrate that cerebral WM volume is affected in a regionally-specific manner with nondemented aging as well as in AD, and that WM changes in AD could contribute to the clinical expression of dementia.

## Methods

### *Participants*

High-resolution structural MR scans were obtained from two sets of participants. Twenty young healthy individuals were imaged on two occasions for assessing test–retest reliability of the parcellation method (TRT; $n$=8M/12F, mean age=23.4) and 299 participants for the examination of volumetric alterations in aging and AD. The main sample of 299 individuals was grouped as younger adults (YNG; individuals younger than 60 years; $n$=62M/73F, mean age=26.5), older adults (OLD; individuals 60 years and older; $n$=26M/47F, mean age=76.8), and individuals with AD (matched to OLD; $n$=37M/54F, mean age=77.6, clinical dementia rating [CDR] (Morris, 1993); 63=0.5 and 28=1; Table 1). The association between age and regional volume was examined across all nondemented individuals, as well as through group comparisons using 60 years of age as the cutoff. This grouping of YNG and OLD was based on prior literature suggesting that WM volume is relatively preserved until late aging and to match the OLD to the AD group.

All OLD and AD were recruited and clinically evaluated through the Washington University Alzheimer's Disease Research Center (ADRC) as reported previously (Berg et al., 1998; Morris, 1993). The YNG adults were recruited from the community as part of ongoing cognitive studies. Individuals were excluded if they exhibited any neurological or psychiatric conditions that could contribute to dementia. OLD individuals were all clinically-screened to show no signs of even mild

**Table 1**
Participant demographics

| Group | *N* | Age (SEM) | CDR[a] 0/.5/1 | MMSE[b] |
|---|---|---|---|---|
| YNG[c] | 135 (62M/73F) | 26.5 (.8) | N/A | N/A |
| OLD[d] | 73 (26M/47F) | 76.8 (.8) | 73/0/0 | 29.0 (25–30) |
| AD[e] | 91 (37M/54F) | 77.6 (.7) | 0/63/28 | 24.5 (14–30) |

[a] CDR: Clinical Dementia Rating.
[b] MMSE: Mini Mental State Examination.
[c] YNG: younger adults.
[d] OLD: older adults.
[e] AD: participants with Alzheimer's disease.

cognitive impairment (all CDR 0). Fotenos et al. (2005) describe the recruitment characteristics of this sample in detail. Participants consented in accordance with guidelines of the Washington University Human Studies Committee.

These data are openly available to the community via the OASIS project (www.oasis.org; Marcus et al., 2007) thanks in part to resources from the Washington University ADRC. This sample overlaps with prior studies examining aging and AD (Andrews-Hanna et al., 2007; Buckner et al., 2005; Dickerson et al., 2008; Fotenos et al., 2005, 2008; He et al., 2008; Head et al., 2004, 2005; Salat et al., 2004).

*MR acquisition and analysis*

Two to five T1-weighted MP-RAGE scans were motion corrected and averaged per participant for image processing on a single scanner (Siemens 1.5-T Vision System, resolution 1×1×1.25 mm, TR=9.7 ms, TE=4 ms, FA=10°, TI=20 ms, TD=500 ms) to create high signal/contrast to noise volumes for each participant. Acquisition parameters were empirically optimized to increase GM/WM/cerebrospinal fluid contrast. Imaging of participants from each group was distributed across time, and there was no overrepresentation of a particular group at any time during imaging.

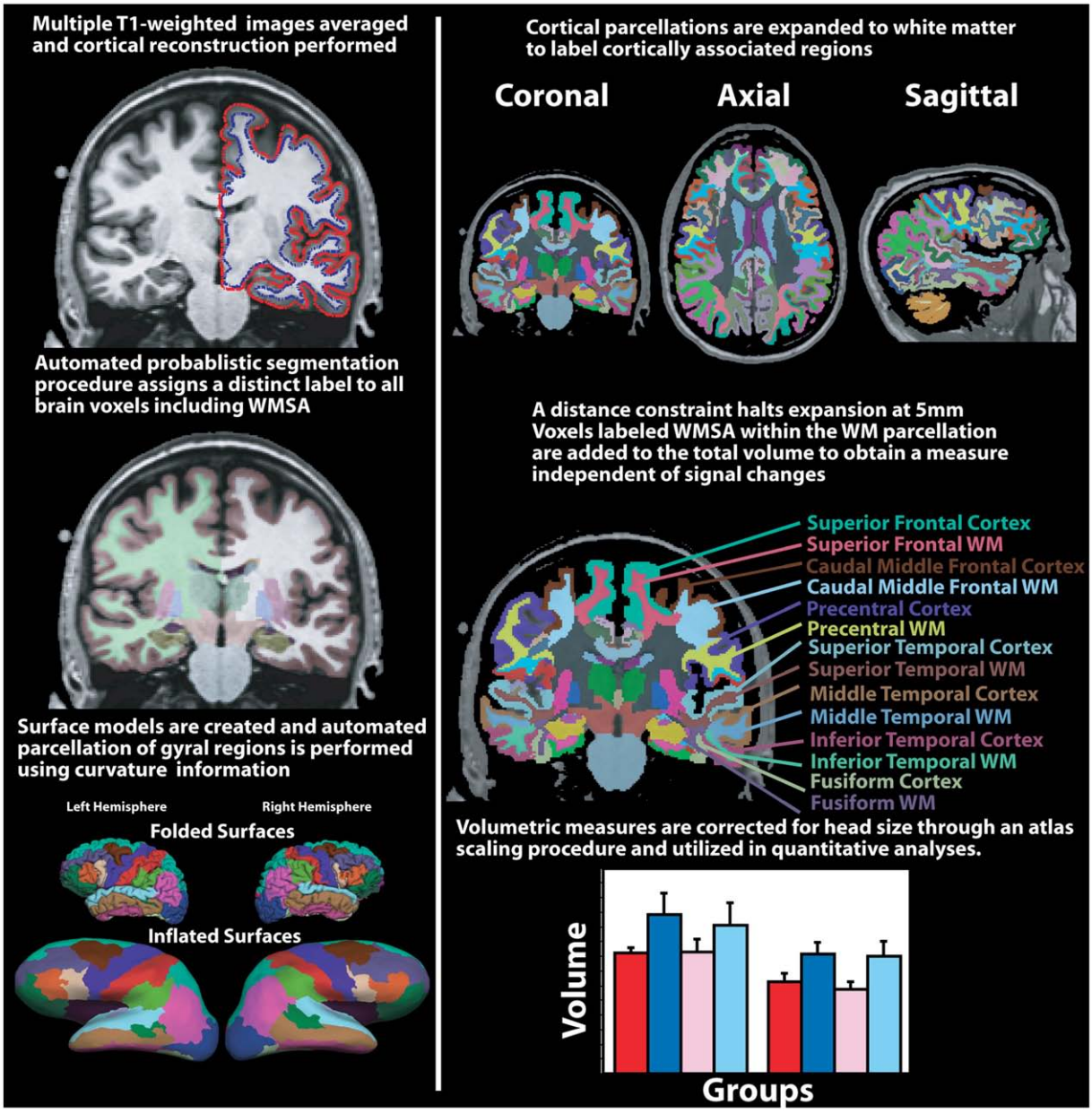


**Fig. 1.** WM parcellation method. The WM parcellation method is an extension of a previously described cortical reconstruction (left panel, top), segmentation (left panel, middle) and parcellation procedure (left panel, bottom) that utilized spherical spatial normalization (Fischl et al., 1999b) to label gyral and sulcal areas throughout the brain (Desikan et al., 2006; Fischl et al., 2004). Cortical parcellations were subsequently used to assign a label to the underlying white matter by the construction of a Voronoi diagram in the WM voxels of the MR volume based on distance to the nearest cortical parcellation label (right panel, top and middle). Each Voronoi polygon then inherited the label of the parcellation unit, yielding a complete labeling of the cerebral WM. Measures were corrected for head size with an atlas-based scaling procedure (Buckner et al., 2004) for quantitative analysis.

**Table 2**
Test–retest reliability

| WM parcellation | Mean % difference (L/R) | Standard deviation (L/R) |
|---|---|---|
| Banks sup temp sulcus | 2.7/2.7 | .03/.02 |
| Caudal anterior cingulate | 6.5/6.4 | .05/.04 |
| Caudal middle frontal | 3.7/2.1 | .04/.02 |
| Cuneus | 3.3/4.1 | .02/.02 |
| Entorhinal | 19.8/16.2 | .08/.09 |
| Fusiform | 4.7/3.5 | .02/.02 |
| Inferior parietal | 2.4/2.6 | .02/.02 |
| Inferior temporal | 7.7/7.8 | .04/.04 |
| Isthmus cingulate | 4.5/7.2 | .04/.06 |
| Lateral occipital | 2.4/2.8 | .02/.02 |
| Lateral orbitofrontal | 2.4/2.2 | .02/.02 |
| Lingual | 3.4/3.6 | .02/.03 |
| Medial orbitofrontal | 7.6/3.6 | .04/.03 |
| Middle temporal | 10.2/6.0 | .06/.03 |
| Parahippocampal | 8.0/3.8 | .04/.03 |
| Paracentral | 2.4/2.0 | .02/.02 |
| Pars opercularis | 5.4/3.3 | .04/.03 |
| Pars orbitalis | 11.3/6.8 | .06/.05 |
| Pars triangularis | 6.9/3.2 | .05/.03 |
| Pericalcarine | 4.0/3.8 | .04/.03 |
| Postcentral | 3.6/2.3 | .03/.02 |
| Posterior cingulate | 6.3/3.6 | .04/.02 |
| Precentral | 3.3/1.8 | .03/.01 |
| Precuneus | 2.1/2.2 | .01/.02 |
| Rostral anterior cingulate | 5.6/5.9 | .04/.07 |
| Rostral middle frontal | 5.0/2.9 | .02/.01 |
| Superior frontal | 4.3/4.4 | .02/.02 |
| Superior parietal | 2.6/2.5 | .02/.02 |
| Superior temporal | 3.6/3.1 | .03/.03 |
| Supramarginal | 2.6/1.6 | .02/.01 |
| Frontal pole | 19.0/10.0 | .15/.12 |
| Temporal pole | 29.7/25.4 | .19/.10 |
| Transverse temporal | 6.7/4.9 | .05/.04 |

Cortical surface models were created as described previously (Dale et al., 1999; Desikan et al., 2006; Fischl et al., 1999a, 2004; Salat et al., 2004). This method utilized intensity and continuity information from the entire three dimensional MR volumes in segmentation and deformation procedures to produce accurate representations of the cortical mantle. The tissue boundaries are determined using spatial intensity gradients and are therefore not simply reliant on absolute signal intensity. After the creation of topologically correct (Fischl et al., 2001) surface models, spherical coordinate procedures (Fischl et al., 1999b) were utilized in cortical surface parcellation which was validated against manual measurements (Desikan et al., 2006; Fischl et al., 2004).

These parcellations were subsequently used to assign a label to the underlying WM by the construction of a Voronoi diagram in the WM voxels based on distance to the nearest cortical parcellation label (Fig. 1). Each Voronoi polygon then inherited the label of the parcellation unit, yielding a complete labeling of the cerebral WM. A distance constraint was applied, halting the label expansion after 5 mm to result in labeling of the gyral WM and to avoid inclusion of WM from the centrum semiovale and periventricular regions (although certain regions in close proximity to the ventricles did contact this structure), and WM voxels beyond this were unlabeled resulting in 'cortically associated' gyral WM volumes. WM signal abnormalities (WMSA; i.e. T1 hypointensities within the WM) were labeled utilizing a probabilistic procedure (Fischl et al., 2002) and included in the total regional WM volume to examine volume changes independent of WMSA burden. However, total WMSA volumes were obtained (as described in Burns et al. (2005)) and the association between this classic imaging measure of WM abnormality and the regional WM volumes was examined for the current study. All regional volumes were corrected for estimated total intracranial volume (eTIV) utilizing an atlas scaling and covariance approach as previously described (Buckner et al., 2004). This method was validated against manual measurements of intracranial volume in prior work (Buckner et al., 2004).

### *Test–retest measurement reliability*

In order to assess the reliability of the WM parcellation procedure, we examined regional volumes from each of the twenty young healthy TRT individuals over two imaging sessions separated by a brief interval during which minimal true biological changes are likely to have occurred. There was a mean delay of 21 days between test and retest sessions (range 1–89 days).

### *Statistical analysis*

The associations between age and regional WM volume were examined by Pearson's correlation and simple and polynomial regression to examine whether curvilinear fits significantly explained the data. Group differences in regional WM volume between OLD and AD were examined by analysis of covariance with regional WM volumes as dependent factors and age as a cofactor. Given the statistical power, we used a moderate statistical threshold and only results with $p<0.01$ were considered. Interactions with $p>0.01$ were removed from the model.

**Table 3**
Association between age and WM volume in all nondemented participants

| WM region | LH *t*-value (Age/Age$^2$) | LH *p*-value (Age/Age$^2$) | RH *t*-value (Age/Age$^2$) | RH *p*-value (Age/Age$^2$) |
|---|---|---|---|---|
| Banks STS | 1.62/−2.00 | 0.107/0.039 | 1.67/−2.40 | 0.097/0.018 |
| Caudal anterior cingulate | −2.28/2.08 | 0.024/0.039 | 0.74/−1.00 | 0.459/0.317 |
| Caudal middle frontal | 0.35/−1.25 | 0.721/0.213 | 1.32/−2.10 | 0.189/0.037 |
| Cuneus | 2.42/−2.63 | 0.016/0.009 | 2.88/−3.12 | 0.004/0.002 |
| Entorhinal | 4.07/−4.57 | <0.001/<0.001 | 3.20/−3.70 | 0.002/<0.001 |
| Fusiform | 2.40/−4.15 | 0.017/<0.001 | 2.54/−4.09 | 0.012/<0.001 |
| Inferior parietal | 1.23/−2.07 | 0.221/0.040 | 3.20/−3.96 | 0.002/<0.001 |
| Inferior temporal | 2.26/−3.39 | 0.025/<0.001 | 0.73/−2.39 | 0.466/0.018 |
| Isthmus cingulate | 2.49/−2.89 | 0.014/0.004 | 2.27/−3.00 | 0.024/0.003 |
| Lateral occipital | 3.60/−4.39 | <0.001/<0.001 | 2.90/−3.66 | 0.004/<0.001 |
| Lateral orbitofrontal | 5.16/−6.40 | <0.001/<0.001 | 5.11/−6.07 | <0.001/<0.001 |
| Lingual | 3.09/−4.05 | 0.002/<0.001 | 2.96/−3.74 | 0.003/<0.001 |
| Medial orbitofrontal | 1.39/−2.64 | 0.166/0.009 | 3.97/−5.40 | <0.001/<0.001 |
| Middle temporal | 1.65/−2.66 | 0.100/0.009 | 2.11/−3.51 | 0.036/<0.001 |
| Parahippocampal | 3.72/−4.35 | <0.001/<0.001 | 2.26/−3.16 | 0.025/0.002 |
| Paracentral | 1.39/−2.16 | 0.170/0.032 | 1.68/−2.29 | 0.094/0.023 |
| Pars opercularis | 2.17/−2.99 | 0.031/0.003 | 1.50/−2.30 | 0.135/0.022 |
| Pars orbitalis | 3.09/−3.71 | 0.002/<0.001 | 2.33/−3.11 | 0.021/0.002 |
| Pars triangularis | 2.96/−3.86 | 0.004/<0.001 | 2.46/−3.19 | 0.015/0.002 |
| Pericalcarine | 2.89/−3.65 | 0.004/<0.001 | 3.46/−3.92 | <0.001/<0.001 |
| Postcentral | 1.98/−2.14 | 0.049/0.033 | 1.64/−2.01 | 0.102/0.045 |
| Posterior cingulate | 1.93/−1.92 | 0.055/0.056 | 1.56/−1.96 | 0.121/0.051 |
| Precentral | 3.36/−3.62 | <0.001/<0.001 | 4.12/−4.27 | <0.001/<0.001 |
| Precuneus | 1.79/−2.72 | 0.075/0.007 | 2.91/−3.81 | 0.004/<0.001 |
| Rostral anterior cingulate | 1.69/−2.29 | 0.093/0.023 | −1.07/0.725 | 0.287/0.469 |
| Rostral middle frontal | 2.23/−2.94 | 0.027/0.004 | 1.72/−2.73 | 0.088/0.007 |
| Superior frontal | 2.64/−4.02 | 0.009/<0.001 | 2.97/−4.62 | 0.003/<0.001 |
| Superior parietal | 1.69/−2.31 | 0.092/0.022 | 1.29/−1.79 | 0.200/0.075 |
| Superior temporal | 3.18/−3.95 | 0.002/<0.001 | 4.13/−5.03 | <0.001/<0.001 |
| Supramarginal | 1.32/−1.82 | 0.190/0.070 | 0.36/−1.03 | 0.718/0.305 |
| Frontal pole | −1.32/0.50 | 0.189/0.615 | 0.90/−1.68 | 0.372/0.094 |
| Temporal pole | 5.07/−5.42 | <0.001/<0.001 | 2.95/−3.42 | 0.004/<0.001 |
| Transverse temporal | 0.25/−0.03 | 0.807/0.974 | 1.38/−1.20 | 0.169/0.233 |

Secondary analyses were performed splitting the groups by sex to determine whether observed effects were replicable across men and women. Additional analyses examined the association between ventricular and regional WM volumes to determine whether WM volume was affected independently of this classical metric of neural integrity.

## Results

### *Test retest measurement reliability*

The results for the test–retest error for each structure are presented in Table 2. Test–retest assessment was based on automated measures without additional corrections or processing. Each measure came from a distinct MR session and thus the error estimates includes real-world sources of variance linked to head positioning and scanner instability. Measurements were generally reliable, with the majority of structures within approximately 5% of the total structure. A small number of structures showed greater measurement variability and were thus examined only as exploratory analyses for the current study. The highlighted results come from regions that show good to excellent test–retest reliability. Certain regions, such as the entorhinal WM, increased in reliability when examined as a combined metric with parahippocampal WM. However, we choose to analyze this structure independently from the parahippocampal WM because the effects measured were reliable across independent samples,

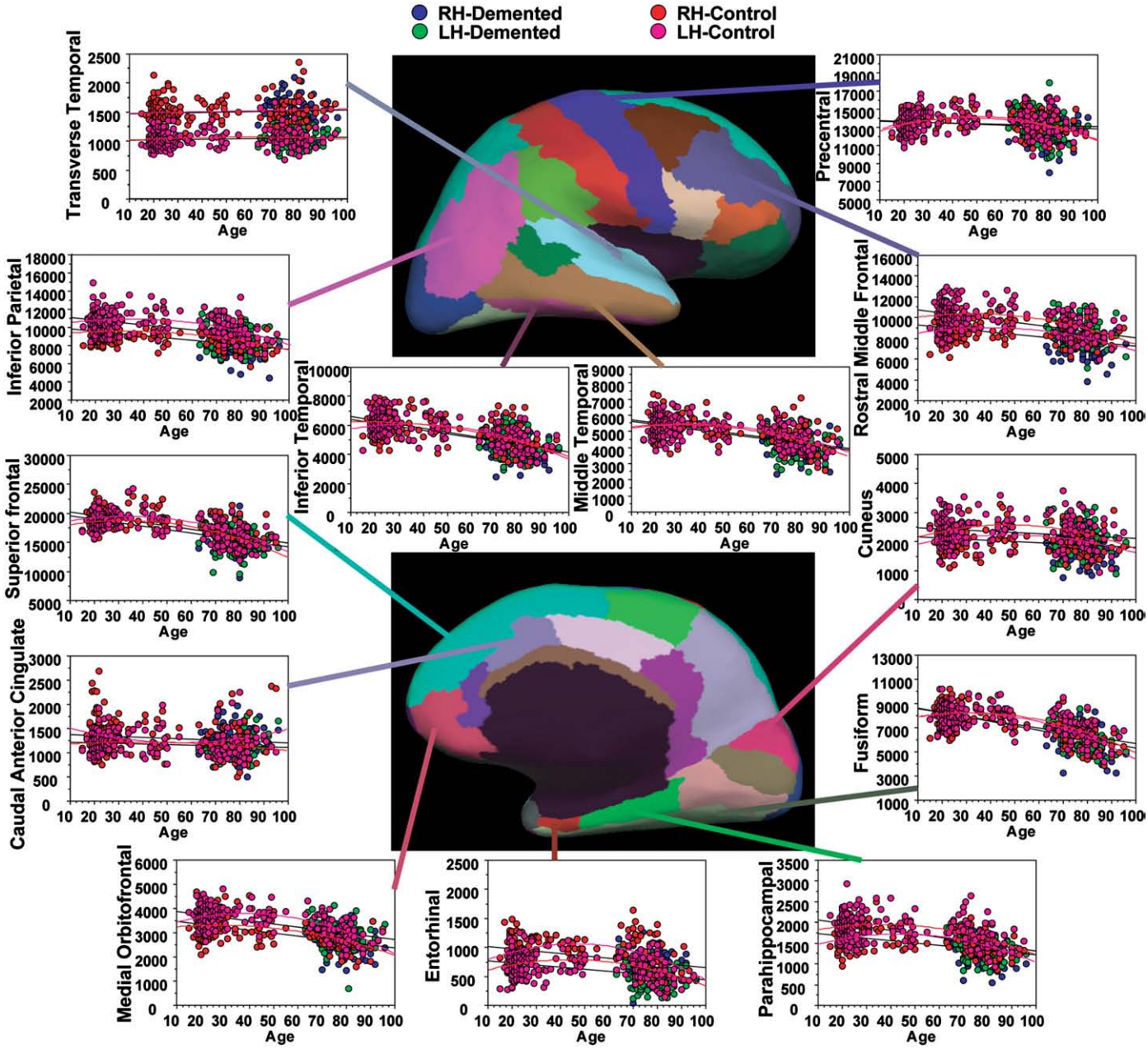


**Fig. 2.** Scatter plots of the volume of selected WM regions by age in nondemented and in demented individuals. There were strong associations between WM volume and age throughout several regions of the brain. Effects of dementia beyond those of age were somewhat more selective and were greatest in regions typically associated with cortical degeneration in studies of AD. See Tables 3 and 4 for a comprehensive list of statistical effects.

demonstrating the ability to detect valid changes regardless of the cross-session reliability.

*Aging*

There were strong associations between WM volume and age in most regions examined in the nondemented individuals with effects in bilateral fusiform, superior frontal, medial orbital frontal, inferior temporal, and middle temporal WM (Table 3; Fig. 2). Of note, an absence of age-associated reduction was found in bilateral caudal anterior cingulate and transverse temporal WM. The majority of regions were significantly fit by a quadratic function. This fit generally exhibited a preservation or rise in volume until approximately the end of the fifth decade, and then, subsequently, a precipitous decline in volume (Table 3; Fig. 2). However a variety of patterns of age-associated change were apparent in the different regions.

*AD*

Effects of AD that exceeded volume reductions linked to aging were found in several regions but were somewhat more selective than those found with the comparison of OLD to YNG. In general, effects of AD tended to be in regions where cortical degeneration has been reported including parahippocampal, entorhinal, precuneus and inferior parietal WM, as well as rostral middle frontal WM (Table 4; Fig. 2). The majority of the WM volume differences were significantly different from nondemented control participants (OLD) when limiting the AD sample to individuals with CDR 0.5 only indicating that WM differences could be detected in the very earliest stages of the disease (Table 4).

We next examined the association between total WM signal abnormalities and regional WM volumes, controlling for age in the OLD and AD combined. There were modest associations between abnormalities and WM volume in the left pars opercularis ($t=2.21$, $p=0.030$), left pars orbitalis ($t=-2.10$, $p=0.038$), left and right postcentral ($t=2.83$, $p=0.006$; $t=2.94$, $p=0.004$, respectively), left precentral ($t=2.84$, $p=0.006$), left and right superior parietal ($t=2.80$, $p=0.006$; $t=2.88$, $p=0.005$, respectively), left transverse temporal ($t=3.20$, $p=0.002$), right banks of the superior temporal sulcus ($t=2.08$, $p=0.040$), right superior temporal ($t=2.32$, $p=0.023$), and right supramarginal WM ($t=2.42$, $p=0.018$).

*Sex effects*

The primary age and AD effects on WM were apparent in both men and women when splitting the groups by sex, demonstrating a replication of the study results in most regions (Fig. 3). Sex differences were apparent in a small number of regions and were generally of minor effect size as contrast to the major effects that

**Table 4**
Reduction in WM volume with AD: ANCOVA for each region covarying for age

| WM region | *F*-value (LH/RH) | *p*-value (LH/RH) | % Difference OLD>AD (LH/RH) |
|---|---|---|---|
| Banks STS | 2.62/8.46 | 0.108/0.004 | 4.06/7.68 |
| Caudal anterior cingulate | 0.74/0.43 | 0.391/0.512 | 2.53/1.75 |
| Caudal middle frontal | 7.35/2.89 | 0.007/0.091 | 2.36/4.13 |
| Cuneus | 8.24/3.03 | 0.004[a]/0.084[a] | 11.07/6.01 |
| Entorhinal | 8.58/24.47 | 0.004[a,b]/<0.001[a] | 21.34/25.86 |
| Fusiform | 4.29/8.20 | 0.040[a]/0.005[a] | 5.62/6.26 |
| Inferior parietal | 16.79/11.68 | <0.001[a]/<0.001[a,b] | 8.25/8.82 |
| Inferior temporal | 15.23/8.52 | <0.001[a]/0.004[a] | 10.75/7.17 |
| Isthmus cingulate | 13.66/9.66 | <0.001[a]/0.002[a] | 7.85/7.39 |
| Lateral occipital | 6.10/2.90 | 0.015[a]/0.090 | 8.04/4.79 |
| Lateral orbitofrontal | 8.89/5.26 | 0.003[a,b]/0.023[a] | 4.29/3.96 |
| Lingual | 14.63/9.82 | <0.001[a]/0.002[a] | 11.92/9.37 |
| Medial orbitofrontal | 0.55/6.23 | 0.461/0.014[b] | 2.36/4.26 |
| Middle temporal | 16.02/9.81 | <0.001[a]/0.002[a,b] | 10.15/7.92 |
| Parahippocampal | 40.09/48.40 | <0.001[a]/<0.001[a] | 16.36/17.14 |
| Paracentral | 0.22/0.28 | 0.641/0.595 | 1.45/−0.89 |
| Pars opercularis | 0.00/4.77 | 0.955/0.031[a] | 0.24/5.77 |
| Pars orbitalis | 1.92/0.71 | 0.168/0.401 | 4.28/2.35 |
| Pars triangularis | 0.19/0.05 | 0.667/0.820 | 1.21/0.95 |
| Pericalcarine | 10.23/9.36 | 0.002[a]/0.003[a] | 12.12/11.13 |
| Postcentral | 5.31/2.89 | 0.023/0.091 | 4.33/3.32 |
| Posterior cingulate | 3.91/0.14 | 0.050/0.708 | 3.88/−0.42 |
| Precentral | 1.22/0.65 | 0.272/0.422 | 1.91/1.24 |
| Precuneus | 18.61/10.10 | <0.001[a]/0.002[a] | 8.41/5.89 |
| Rostral anterior cingulate | 1.20/0.10 | 0.275/0.749 | 2.57/−1.24 |
| Rostral middle frontal | 23.80/5.34 | <0.001[a]/0.022 | 9.57/4.75 |
| Superior frontal | 9.66/5.55 | 0.002/0.020 | 5.74/4.25 |
| Superior parietal | 9.90/6.49 | 0.002[a]/0.012 | 6.07/5.15 |
| Superior temporal | 1.20/0.63 | 0.275/0.427 | 2.23/1.38 |
| Supramarginal | 16.27/2.41 | <0.001[a]/0.123 | 6.83/2.62 |
| Frontal pole | 0.451/0.04 | 0.503/0.839 | 2.49/0.86 |
| Temporal pole | 11.74/7.59 | 0.001[a]/0.007[a] | 15.47/11.10 |
| Transverse temporal | 0.05/0.07 | 0.831/0.786 | 0.61/0.26 |

[a] Unpaired comparison of OLD to CDR .5 AD alone $p<0.05$.
[b] Regions showing a significant group by age interaction.

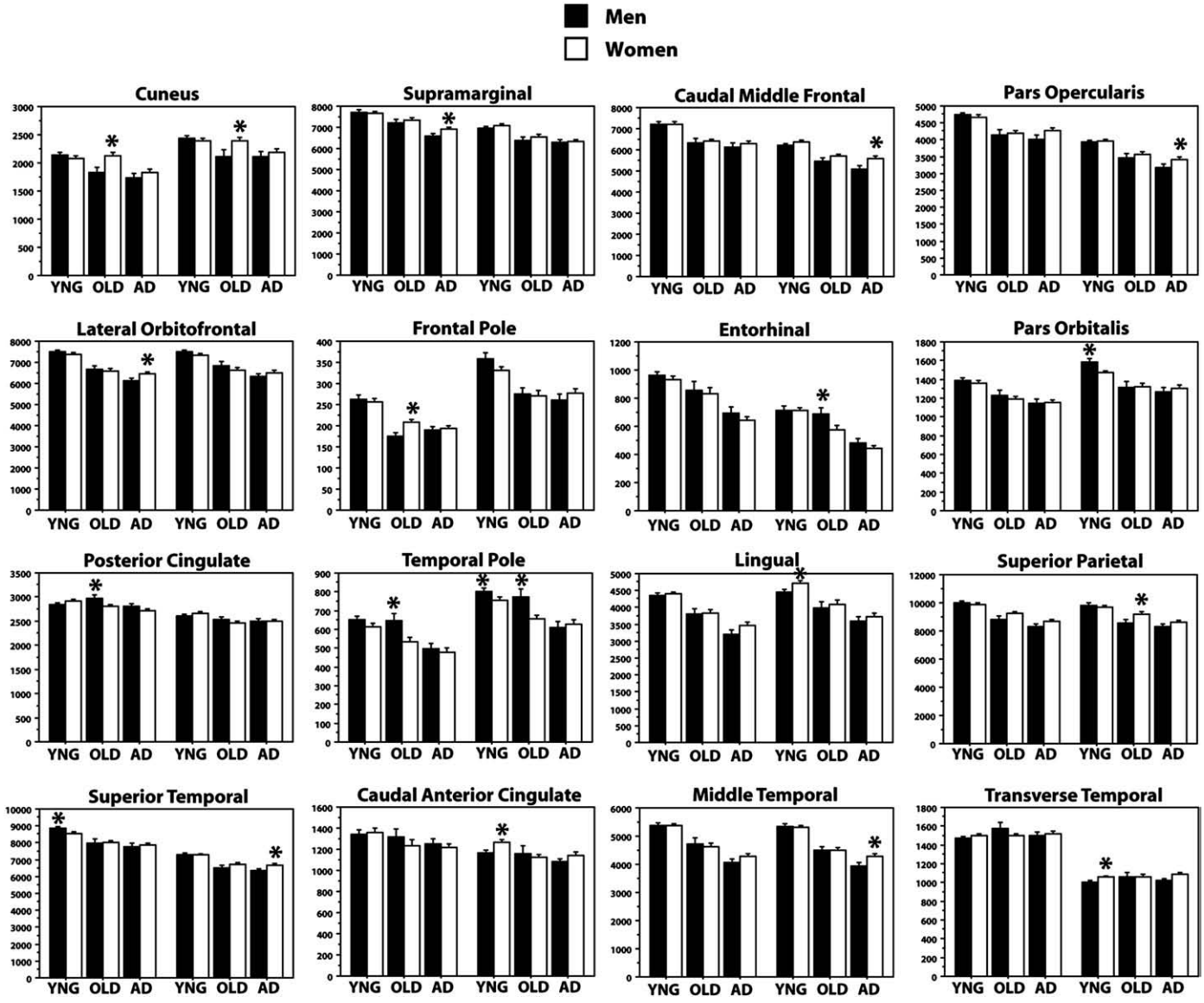


**Fig. 3.** Effects of age and dementia on WM volume split by sex and hemisphere in selected regions. All regions showing a sex differences in WM volumes within any of the three groups are presented. Most effects described in the whole group analyses were replicated across both men and women. There were relatively few regions that demonstrated a difference between men and women or interaction.

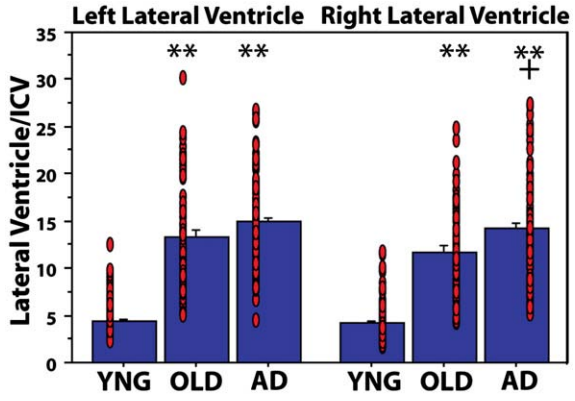


**Fig. 4.** Ventricular volumes in YNG, OLD and AD. There was ventricular enlargement in OLD and AD compared to YNG (**$p<0.001$ compared to YNG) and in AD compared to OLD (+$p<0.005$ compared to OLD). Red circles represent individual participant datapoints.

generalized across male and female participants. Specifically, we examined whether there were sex differences in any region in YNG, OLD, and AD, with each group first examined individually, and secondarily, examined for group interactions. YNG men had greater WM volume in left superior temporal and right temporal pole and pars orbitalis, and less volume in left frontal pole, right caudal anterior cingulate, lingual, and transverse temporal WM compared to YNG women (all $ps<0.05$). OLD men had greater WM volume than OLD women in left posterior cingulate, right entorhinal, and bilateral temporal pole, and less volume in left frontal pole, right superior parietal, and bilateral cuneus (all $ps<0.05$). AD men had greater WM volume than AD women in left and less volume in left lateral orbitofrontal, supramarginal, and right superior temporal, right caudal middle frontal, right middle temporal, and right pars opercularis (all $ps<0.05$). Only the left lateral orbitofrontal, left

**Table 5**
Association between ventricular volume and regional WM volumes

| WM region | YNG-LH | | YNG-RH | | OLD-LH | | OLD-RH | | AD-LH | | AD-RH | |
|---|---|---|---|---|---|---|---|---|---|---|---|---|
| | *r*/*p* | | *r*/*p* | | *r*/*p* | | *r*/*p* | | *r*/*p* | | *r*/*p* | |
| Banks STS | 0.18 | 0.041 | 0.30 | 0.000 | −0.20 | 0.090 | −0.21 | 0.068 | 0.25 | 0.015 | −0.08 | 0.480 |
| Caudal anterior cingulate | −0.20 | 0.019 | −0.11 | 0.184 | −0.08 | 0.480 | 0.03 | 0.812 | −0.26 | 0.012 | 0.10 | 0.331 |
| Caudal middle frontal | 0.02 | 0.832 | −0.19 | 0.026 | −0.08 | 0.481 | −0.24 | 0.042 | −0.12 | 0.256 | −0.18 | 0.092 |
| Cuneus | −0.02 | 0.777 | 0.05 | 0.604 | −0.46 | 0.000 | −0.40 | 0.000 | −0.22 | 0.037 | −0.20 | 0.063 |
| Entorhinal | −0.12 | 0.167 | −0.04 | 0.629 | −0.48 | 0.000 | −0.32 | 0.006 | −0.25 | 0.019 | −0.32 | 0.002 |
| Fusiform | −0.13 | 0.137 | −0.18 | 0.037 | −0.46 | 0.000 | −0.52 | 0.000 | −0.31 | 0.003 | −0.40 | 0.000 |
| Inferior parietal | 0.00 | 0.986 | 0.16 | 0.063 | −0.16 | 0.166 | −0.29 | 0.013 | −0.07 | 0.536 | −0.38 | 0.000 |
| Inferior temporal | −0.05 | 0.565 | −0.07 | 0.452 | −0.41 | 0.000 | −0.52 | 0.000 | −0.11 | 0.281 | −0.40 | 0.000 |
| Isthmus cingulate | −0.04 | 0.655 | −0.05 | 0.592 | −0.39 | 0.001 | −0.32 | 0.006 | −0.29 | 0.005 | −0.18 | 0.082 |
| Lateral occipital | 0.09 | 0.299 | −0.03 | 0.759 | −0.32 | 0.006 | −0.41 | 0.000 | −0.08 | 0.424 | −0.12 | 0.268 |
| Lateral orbitofrontal | −0.11 | 0.212 | −0.17 | 0.046 | −0.41 | 0.000 | −0.41 | 0.000 | −0.18 | 0.089 | −0.28 | 0.008 |
| Lingual | −0.09 | 0.311 | −0.11 | 0.202 | −0.46 | 0.000 | −0.36 | 0.002 | −0.23 | 0.026 | −0.24 | 0.021 |
| Medial orbitofrontal | −0.15 | 0.087 | −0.03 | 0.717 | −0.40 | 0.000 | −0.48 | 0.000 | −0.20 | 0.054 | −0.25 | 0.018 |
| Middle temporal | 0.15 | 0.081 | 0.17 | 0.044 | −0.19 | 0.107 | −0.35 | 0.003 | −0.09 | 0.406 | 0.01 | 0.895 |
| Parahippocampal | −0.14 | 0.110 | 0.06 | 0.520 | −0.48 | 0.000 | −0.44 | 0.000 | −0.34 | 0.001 | −0.26 | 0.014 |
| Paracentral | −0.03 | 0.754 | 0.03 | 0.735 | −0.27 | 0.023 | −0.18 | 0.138 | −0.32 | 0.002 | −0.30 | 0.005 |
| Pars opercularis | −0.10 | 0.240 | −0.02 | 0.778 | −0.48 | 0.000 | −0.37 | 0.001 | −0.17 | 0.099 | −0.22 | 0.037 |
| Pars orbitalis | −0.12 | 0.182 | −0.03 | 0.725 | −0.34 | 0.003 | −0.41 | 0.000 | −0.20 | 0.063 | −0.03 | 0.798 |
| Pars triangularis | −0.10 | 0.231 | 0.00 | 0.964 | −0.55 | 0.000 | −0.29 | 0.014 | −0.34 | 0.001 | −0.14 | 0.175 |
| Pericalcarine | −0.21 | 0.015 | −0.12 | 0.174 | −0.55 | 0.000 | −0.32 | 0.005 | −0.32 | 0.002 | −0.27 | 0.009 |
| Postcentral | −0.05 | 0.594 | 0.09 | 0.274 | −0.45 | 0.000 | −0.36 | 0.002 | −0.28 | 0.008 | −0.03 | 0.757 |
| Posterior cingulate | 0.07 | 0.417 | 0.10 | 0.260 | −0.07 | 0.534 | −0.14 | 0.242 | −0.28 | 0.008 | −0.01 | 0.961 |
| Precentral | −0.01 | 0.930 | 0.08 | 0.383 | −0.37 | 0.001 | −0.32 | 0.006 | −0.17 | 0.115 | −0.22 | 0.035 |
| Precuneus | −0.05 | 0.538 | −0.08 | 0.352 | −0.48 | 0.000 | −0.48 | 0.000 | −0.45 | 0.000 | −0.33 | 0.001 |
| Rostral anterior cingulate | 0.07 | 0.427 | −0.08 | 0.369 | −0.18 | 0.119 | 0.18 | 0.127 | 0.18 | 0.095 | −0.09 | 0.383 |
| Rostral middle frontal | −0.01 | 0.937 | 0.07 | 0.424 | −0.29 | 0.012 | −0.35 | 0.002 | −0.16 | 0.123 | −0.21 | 0.048 |
| Superior frontal | −0.11 | 0.202 | 0.03 | 0.716 | −0.51 | 0.000 | −0.52 | 0.000 | −0.44 | 0.000 | −0.41 | 0.000 |
| Superior parietal | −0.18 | 0.032 | 0.09 | 0.319 | −0.32 | 0.005 | −0.33 | 0.004 | −0.14 | 0.174 | −0.09 | 0.406 |
| Superior temporal | −0.11 | 0.203 | 0.00 | 0.963 | −0.48 | 0.000 | −0.46 | 0.000 | −0.25 | 0.016 | −0.06 | 0.543 |
| Supramarginal | −0.12 | 0.162 | −0.15 | 0.091 | −0.30 | 0.009 | −0.35 | 0.002 | −0.25 | 0.016 | −0.12 | 0.260 |
| Frontal pole | 0.04 | 0.657 | −0.02 | 0.776 | −0.29 | 0.013 | 0.00 | 0.995 | 0.12 | 0.262 | −0.16 | 0.136 |
| Temporal pole | −0.01 | 0.894 | −0.12 | 0.172 | −0.17 | 0.140 | −0.15 | 0.213 | 0.01 | 0.901 | −0.13 | 0.211 |
| Transverse temporal | −0.28 | 0.001 | −0.10 | 0.241 | 0.03 | 0.780 | −0.03 | 0.802 | −0.20 | 0.057 | −0.11 | 0.308 |

posterior cingulate, and bilateral cuneus showed a significant groups by sex interaction overall (all $ps<0.05$).

*Ventricular volume*

Ventricular enlargement is an additional potential index of WM alterations. Fig. 4 demonstrates ventricular enlargement in OLD compared to YNG (left and right $ps<0.001$) and in AD compared to OLD (left and right $ps=0.07$ and 0.003, respectively; Fig. 4). Table 5 presents the association between regional WM volumes and ventricular volume in each hemisphere. There were minimal associations between ventricular and WM volume in YNG, several regional associations in OLD, and a selective set of associations in AD which were mostly found in a subset of the regions showing associations in the OLD.

## Discussion

The current study demonstrated patterns of WM atrophy in normal older adults and in patients with AD utilizing a novel, automated WM parcellation procedure. These data reveal that widespread differences in WM volume are a consequence of late, nondemented aging and that additional WM volume reduction beyond the effects of age is significant, yet somewhat more regionally selective, in AD. Profound age-associated WM differences were found in regions typically thought to be affected by age such as portions of the frontal lobe including medial orbitofrontal WM, a region that has been found to show accelerated diffusion changes in an independent sample in our prior work (Salat et al., 2005a,b). The novel procedure revealed information that has not been reported in prior work. For example, although WM atrophy was apparent in regions often described to be affected with aging, significant reductions in volume were also found in regions that have not been widely previously reported, such as fusiform, inferior temporal, and middle temporal WM. Such findings may not have been possible when examining data on a lobar basis. Certain regions such as superior frontal gyrus showed WM atrophy with age as well as cortical thinning in our prior work (Salat et al., 2004). These findings may suggest a preferential vulnerability of the superior frontal gyrus to the effects of aging although the general pattern of age-associated WM atrophy is best described as being wide-spread. Some cortical areas demonstrated evidence of preserved or even increased volume in the younger adults into the sixth decade, with a precipitous decline thereafter. These results suggest that regional WM volume is dynamically changing throughout the adult age span and may exhibit complex patterns of growth and decline.

Strong effects were apparent in some regions that have not typically been noted in prior studies of aging, such as the fusiform WM. However, recent work by Thomas et al. found an age associated reduction in diffusion metrics in regions within the fusiform that was associated with a decline in facial perception in older adults (Thomas et al., 2008). These findings provide converging evidence of the effects

measured with the WM parcellation technique and the potential importance of such procedures for broadly exploring the brain in a regionally unbiased manner.

Effects of AD were greatest in areas associated with cortical degeneration including entorhinal, parahippocampal, and posterior cingulated/precuneus WM, and show some overlap with our prior work examining cortical degeneration in AD (Dickerson et al., 2008). These effects remained when limiting the sample to individuals with a CDR 0.5 (Table 4), suggesting that WM changes occur relatively early with regard to clinical presentation. Similarly, patterns of WM degeneration with aging showed some overlap (e.g. superior frontal gyrus) and some distinct effects (e.g. fusiform) compared to our prior work on age-associated cortical loss (Salat et al., 2004). Patterns of age and AD associated WM atrophy differed, yet there was some convergence between these conditions in the vulnerability of superior frontal, middle temporal, and inferior temporal WM.

Overall, these data demonstrate the potential role of regional WM changes in age and AD associated neural and cognitive decline. One possibility is that WM degeneration contributes to the overall reduction in integrity of cognitive networks that are affected in the earliest stages of AD. These alterations could contribute to the classically described isolation of the hippocampal formation from the neocortex (Hyman et al., 1984), as also demonstrated in our recent diffusion work (Salat et al., 2008), and to the profound memory symptoms that are evident in the earliest stages of clinically recognizable AD. Recent functional imaging studies have revealed a more extensive network important to memory function that includes the hippocampal formation and specific, distributed cortical regions linked to the hippocampal formation (Buckner et al., 2008; Vincent et al., 2006; Wagner et al., 2005). WM volume in AD was reduced throughout many of these regions consistent with AD being linked to disruption of a broad network (Buckner et al., 2008; He et al., 2008; Salat et al., 2008). Given the finding that WM volume loss is apparent with very mild dementia, it is possible that this loss could have an important impact on clinical status, and could explain a portion of the variability in clinical presentation.

A number of findings uphold the utility of the presented WM parcellation method for labeling homologous regions across individuals. Test–retest reliability across two scan sessions in twenty individuals was generally good, with the majority of regions being within 5%. Variance in the volumetric measures was low across young and older adults, as well as across patients with AD. Data showed expected directional age and disease related changes. Certain findings of age and AD-related volume reduction measured using this technique are in accord with our prior studies of WM volume loss as well as DTI anisotropy studies of WM integrity (Head et al., 2004; Salat et al., 2005a,b, 2008). There were associations between WMSA volume and regional WM volumes, which may suggest that volume loss is in some way associated with pathological mechanisms contributing to these lesions. However, these were modest effects, and the relative lack of associations overall may suggest that these volumetric measures provide indices of additional independent pathologic processes as has been demonstrated in prior work (Smith et al., 2000). In contrast, there were regional associations between WM volume and ventricular volume in the OLD and AD suggesting that these regional measurements of WM volume could provide further insight into the clinical implications of ventricular enlargement which has been traditionally fairly non-specific with regard to disease pathology. Future studies will examine this in greater detail, as well as the relationship between WM atrophy and cortical thickness to better understand the relationship between these distinct markers of degeneration. Sex differences in volumetric measures were minimal in each of the three groups, and differences found were not consistent across groups or across hemispheres, suggesting that gender has a relatively minor influence on the described measures.

Certain prior imaging and post mortem studies have noted limited or total lack of change in WM volume in aging or AD (Double et al., 1996; Jernigan et al., 1991a,b; Obara et al., 1994; Rusinek et al., 1991; Sullivan et al., 1995; Tanabe et al., 1997). We find preservation of WM volume in the early portion of the adult age span, and only selective regional loss of WM volume with AD. Additionally, the data suggest that younger AD may show greater regional WM volume differences compared to age matched controls compared to older AD (see Fig. 2). Such an effect could make the detection of WM volume loss more difficult in smaller participant samples or with examination of a limited portion of the age span. These data demonstrate the importance of a full adult agespan study of regional effects due to the complex regional patterns measured.

It should be noted that the present WM parcellation scheme is an extension of cortical parcellation procedures. In this sense, any variation in the methods for cortical parcellation could affect the overall WM measures. For example, changes in surface area of a cortical region would affect the amount of WM labeled. It is also possible that changes in tissue composition could affect surface placement and volume measurements. A portion of the temporal lobe regions showed reduced cross-session reliability, particularly in the smaller regions. We note that that the effects were generally reliable across regions. That is, most of the effects reported were replicated in the two samples examined (men and women) across groups. Additionally, combining across regions, for example, combining the entorhinal and parahippocampal regions, improves reliability without changing the interpretation of the results. It is therefore likely that the results presented are not substantially altered by the cross-session reliability. However, future work examining the longitudinal nature of WM volume loss will require further development to enhance this reliability. The procedures for surface generation utilize local intensity gradient information (Dale et al., 1999; Fischl and Dale, 2000; Fischl et al., 1999a, 2001), and thus, should not be greatly affected by absolute intensity changes as long as contrast between the two tissue classes (GM and WM) still remains. The participant sample overlaps partially with our prior work, and the finding of decreases in WM volume in certain regions that also showed cortical thinning, such as the superior frontal gyrus, suggest that the WM volume reduction measured is not a result of surface misplacement in the cortical reconstruction. We also note that the specific technical procedures used here may influence the measurements. For example, the cortical parcellation regions designate the labeling of the WM, and it is possible that different anatomical schemes would produce varying results. The Freesurfer tools for the parcellation procedure are freely available for download (surfer.nmr.mgh.harvard.edu), and therefore, investigators could examine the reproducibility of the results in independent datasets such as the Alzheimer's Disease Neuroimaging Initiative (ADNI; www.adni-info.org/) and also against alternative parcellation schemes. The data examined here are also freely available through the OASIS data release (Marcus et al., 2007; http://www.oasis-brains.org/) allowing future investigators to contrast and improve upon all aspects of the present study. The present study demonstrates differential patterns of WM degeneration in aging and dementia and it is possible that WM degeneration may contribute to cognitive decline and dementia severity in AD.

## Acknowledgments

This work was supported by NCRR P41RR14075, the MIND Institute, the Athinoula A. Martinos Center for Biomedical Imaging, NINR NR010827, NIA AG024898, AG05886, AG05681, HHMI, HBP NS39581 and RR14075. We thank the Washington University ADRC for making MRI data available.

## Appendix A

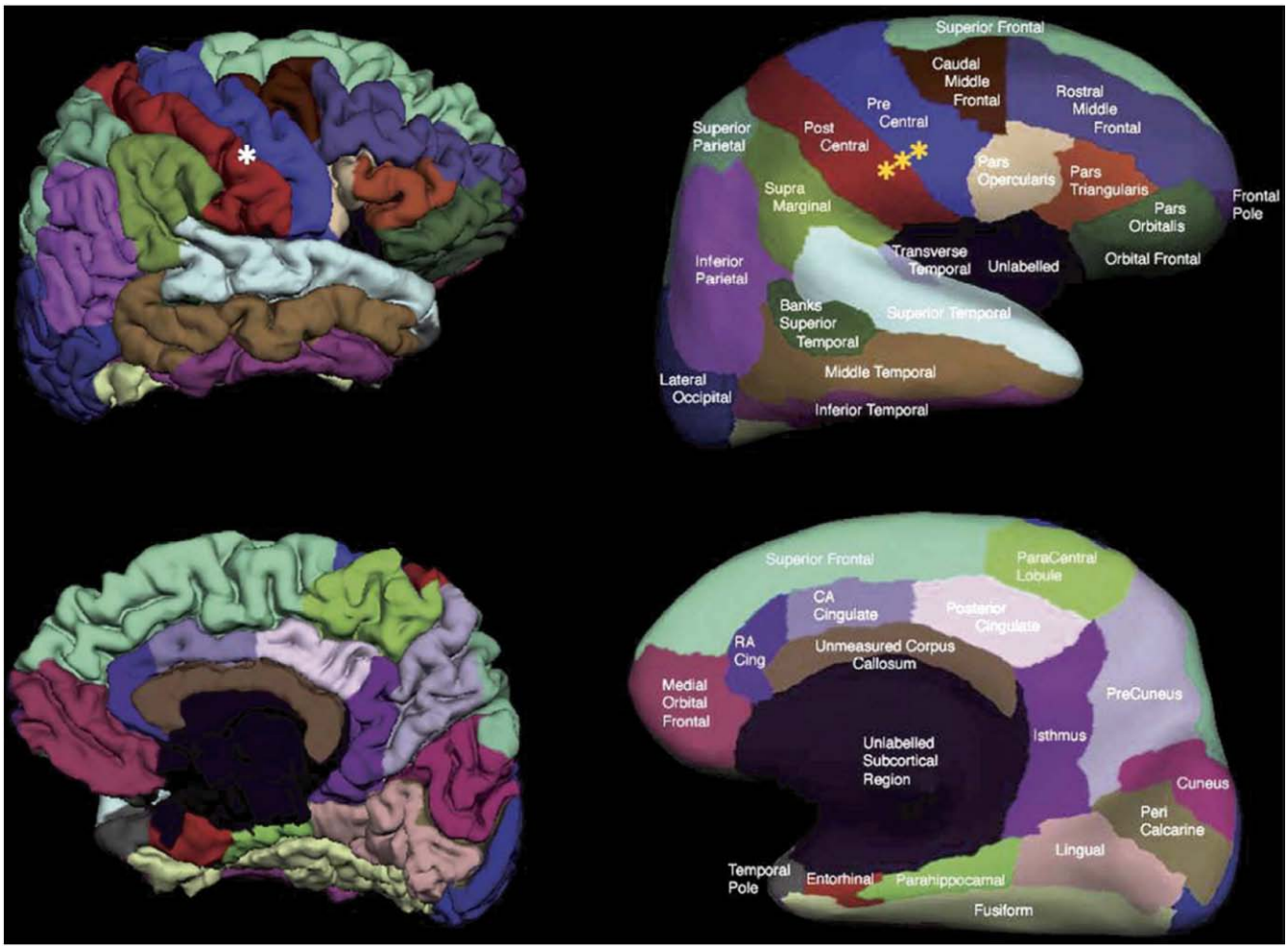


**Fig. A1.** Reprinted from Desikan et al. (2006). A demonstration of the cortical parcellation scheme on the folded (left) and inflated (right) cortical surface with the name of each parcellation unit overlaid.

## References


Anderson, J.M., Hubbard, B.M., Coghill, G.R., Slidders, W., 1983. The effect of advanced old age on the neurone content of the cerebral cortex. Observations with an automatic image analyser point counting method. J. Neurol. Sci. 58, 235–246.

Andrews-Hanna, J.R., Snyder, A.Z., Vincent, J.L., Lustig, C., Head, D., Raichle, M.E., Buckner, R.L., 2007. Disruption of large-scale brain systems in advanced aging. Neuron 56, 924–935.

Armstrong, C.L., Traipe, E., Hunter, J.V., Haselgrove, J.C., Ledakis, G.E., Tallent, E.M., Shera, D., van Buchem, M.A., 2004. Age-related, regional, hemispheric, and medial–lateral differences in myelin integrity in vivo in the normal adult brain. AJNR Am. J. Neuroradiol. 25, 977–984.

Bartzokis, G., Beckson, M., Lu, P.H., Nuechterlein, K.H., Edwards, N., Mintz, J., 2001. Age-related changes in frontal and temporal lobe volumes in men: a magnetic resonance imaging study. Arch. Gen. Psychiatry 58, 461–465.

Bartzokis, G., Cummings, J.L., Sultzer, D., Henderson, V.W., Nuechterlein, K.H., Mintz, J., 2003. White matter structural integrity in healthy aging adults and patients with Alzheimer disease: a magnetic resonance imaging study. Arch. Neurol. 60, 393–398.

Berg, L., McKeel Jr., D.W., Miller, J.P., Storandt, M., Rubin, E.H., Morris, J.C., Baty, J., Coats, M., Norton, J., Goate, A.M., Price, J.L., Gearing, M., Mirra, S.S., Saunders, A.M., 1998. Clinicopathologic studies in cognitively healthy aging and Alzheimer's disease: relation of histologic markers to dementia severity, age, sex, and apolipoprotein E genotype. Arch. Neurol. 55, 326–335.

Bigler, E.D., Anderson, C.V., Blatter, D.D., 2002. Temporal lobe morphology in normal aging and traumatic brain injury. AJNR Am. J. Neuroradiol. 23, 255–266.

Bozzali, M., Falini, A., Franceschi, M., Cercignani, M., Zuffi, M., Scotti, G., Comi, G., Filippi, M., 2002. White matter damage in Alzheimer's disease assessed in vivo using diffusion tensor magnetic resonance imaging. J. Neurol. Neurosurg. Psychiatry 72, 742–746.

Braak, H., Braak, E., 1989. Cortical and subcortical argyrophilic grains characterize a disease associated with adult onset dementia. Neuropathol. Appl. Neurobiol. 15, 13–26.

Brickman, A.M., Habeck, C., Zarahn, E., Flynn, J., Stern, Y., 2007. Structural MRI covariance patterns associated with normal aging and neuropsychological functioning. Neurobiol. Aging 28, 284–295.

Buckner, R.L., Head, D., Parker, J., Fotenos, A.F., Marcus, D., Morris, J.C., Snyder, A.Z., 2004. A unified approach for morphometric and functional data analysis in young, old, and demented adults using automated atlas-based head size normalization: reliability and validation against manual measurement of total intracranial volume. NeuroImage 23, 724–738.

Buckner, R.L., Snyder, A.Z., Shannon, B.J., LaRossa, G., Sachs, R., Fotenos, A.F., Sheline, Y.I., Klunk, W.E., Mathis, C.A., Morris, J.C., Mintun, M.A., 2005. Molecular, structural, and functional characterization of Alzheimer's disease: evidence for a relationship between default activity, amyloid, and memory. J. Neurosci. 25, 7709–7717.

Buckner, R.L., Andrews-Hanna, J.R., Schacter, D.L., 2008. The brain's default network: anatomy, function, and relevance to disease. Ann. N. Y. Acad. Sci. 1124, 1–38.

Burns, J.M., Church, J.A., Johnson, D.K., Xiong, C., Marcus, D., Fotenos, A.F., Snyder, A.Z., Morris, J.C., Buckner, R.L., 2005. White matter lesions are prevalent but differentially related with cognition in aging and early Alzheimer disease. Arch. Neurol. 62, 1870–1876.

Choi, S.J., Lim, K.O., Monteiro, I., Reisberg, B., 2005. Diffusion tensor imaging of frontal white matter microstructure in early Alzheimer's disease: a preliminary study. J. Geriatr. Psychiatry Neurol. 18, 12–19.

Christiansen, P., Larsson, H.B., Thomsen, C., Wieslander, S.B., Henriksen, O., 1994. Age dependent white matter lesions and brain volume changes in healthy volunteers. Acta Radiol. 35, 117–122.

Dale, A.M., Fischl, B., Sereno, M.I., 1999. Cortical surface-based analysis. I. Segmentation and surface reconstruction. NeuroImage 9, 179–194.

de Leeuw, F.E., de Groot, J.C., Achten, E., Oudkerk, M., Ramos, L.M., Heijboer, R., Hofman, A., Jolles, J., van Gijn, J., Breteler, M.M., 2001. Prevalence of cerebral white matter lesions in elderly people: a population based magnetic resonance imaging study. The Rotterdam Scan Study. J. Neurol. Neurosurg. Psychiatry 70, 9–14.

de Leon, M.J., George, A.E., Reisberg, B., Ferris, S.H., Kluger, A., Stylopoulos, L.A., Miller, J.D., La Regina, M.E., Chen, C., Cohen, J., 1989. Alzheimer's disease: longitudinal CT studies of ventricular change. AJR Am. J. Roentgenol. 152, 1257–1262.

DeCarli, C., Murphy, D.G., Tranh, M., Grady, C.L., Haxby, J.V., Gillette, J.A., Salerno, J.A., Gonzales-Aviles, A., Horwitz, B., Rapoport, S.I., et al., 1995. The effect of white matter hyperintensity volume on brain structure, cognitive performance, and cerebral metabolism of glucose in 51 healthy adults. Neurology 45, 2077–2084.

DeCarli, C., Grady, C.L., Clark, C.M., Katz, D.A., Brady, D.R., Murphy, D.G., Haxby, J.V., Salerno, J.A., Gillette, J.A., Gonzalez-Aviles, A., Rapoport, S.I., 1996. Comparison of positron emission tomography, cognition, and brain volume in Alzheimer's disease with and without severe abnormalities of white matter. J. Neurol. Neurosurg. Psychiatry 60, 158–167.

Desikan, R.S., Segonne, F., Fischl, B., Quinn, B.T., Dickerson, B.C., Blacker, D., Buckner, R.L., Dale, A.M., Maguire, R.P., Hyman, B.T., Albert, M.S., Killiany, R.J., 2006. An automated labeling system for subdividing the human cerebral cortex on MRI scans into gyral based regions of interest. NeuroImage 31, 968–980.

Dickerson, B.C., Bakkour, A., Salat, D.H., Feczko, E., Pacheco, J., Greve, D.N., Grodstein, F., Wright, C.I., Blacker, D., Rosas, H.D., Sperling, R.A., Atri, A., Growdon, J.H., Hyman, B.T., Morris, J.C., Fischl, B., Buckner, R.L., 2008. The cortical signature of Alzheimer's disease: regionally specific cortical thinning relates to symptom severity in very mild to mild AD dementia and is detectable in asymptomatic amyloid-positive individuals. Cereb. Cortex (2008 July 16, Electronic publication ahead of print).

Double, K.L., Halliday, G.M., Kril, J.J., Harasty, J.A., Cullen, K., Brooks, W.S., Creasey, H., Broe, G.A., 1996. Topography of brain atrophy during normal aging and Alzheimer's disease. Neurobiol. Aging 17, 513–521.

Fischl, B., Dale, A.M., 2000. Measuring the thickness of the human cerebral cortex from magnetic resonance images. Proc. Natl. Acad. Sci. U. S. A. 97, 11050–11055.

Fischl, B., Sereno, M.I., Dale, A.M., 1999a. Cortical surface-based analysis. II: inflation, flattening, and a surface-based coordinate system. NeuroImage 9, 195–207.

Fischl, B., Sereno, M.I., Tootell, R.B., Dale, A.M., 1999b. High-resolution intersubject averaging and a coordinate system for the cortical surface. Hum. Brain Mapp. 8, 272–284.

Fischl, B., Liu, A., Dale, A.M., 2001. Automated manifold surgery: constructing geometrically accurate and topologically correct models of the human cerebral cortex. IEEE Trans. Med. Imag. 20, 70–80.

Fischl, B., Salat, D.H., Busa, E., Albert, M., Dieterich, M., Haselgrove, C., van der Kouwe, A., Killiany, R., Kennedy, D., Klaveness, S., Montillo, A., Makris, N., Rosen, B., Dale, A.M., 2002. Whole brain segmentation: automated labeling of neuroanatomical structures in the human brain. Neuron 33, 341–355.

Fischl, B., van der Kouwe, A., Destrieux, C., Halgren, E., Segonne, F., Salat, D.H., Busa, E., Seidman, L.J., Goldstein, J., Kennedy, D., Caviness, V., Makris, N., Rosen, B., Dale, A.M., 2004. Automatically parcellating the human cerebral cortex. Cereb. Cortex 14, 11–22.

Fotenos, A.F., Snyder, A.Z., Girton, L.E., Morris, J.C., Buckner, R.L., 2005. Normative estimates of cross-sectional and longitudinal brain volume decline in aging and AD. Neurology 64, 1032–1039.

Fotenos, A.F., Mintun, M.A., Snyder, A.Z., Morris, J.C., Buckner, R.L., 2008. Brain volume decline in aging: evidence for a relation between socioeconomic status, preclinical Alzheimer disease, and reserve. Arch. Neurol. 65, 113–120.

Gado, M., Danziger, W.L., Chi, D., Hughes, C.P., Coben, L.A., 1983. Brain parenchymal density measurements by CT in demented subjects and normal controls. Radiology 147, 703–710.

Good, C.D., Johnsrude, I.S., Ashburner, J., Henson, R.N., Friston, K.J., Frackowiak, R.S., 2001. A voxel-based morphometric study of ageing in 465 normal adult human brains. NeuroImage 14, 21–36.

Guttmann, C.R., Jolesz, F.A., Kikinis, R., Killiany, R.J., Moss, M.B., Sandor, T., Albert, M.S., 1998. White matter changes with normal aging. Neurology 50, 972–978.

Hanyu, H., Sakurai, H., Iwamoto, T., Takasaki, M., Shindo, H., Abe, K., 1998. Diffusion-weighted MR imaging of the hippocampus and temporal white matter in Alzheimer's disease. J. Neurol. Sci. 156, 195–200.

Hashimoto, N., Takeuchi, T., Ishihara, R., Ukai, K., Kobayashi, H., Iwata, H., Iwai, K., Mizuno, Y., Yamaguchi, H., Shibayama, H., 2003. Glial fibrillary tangles in diffuse neurofibrillary tangles with calcification. Acta Neuropathol. (Berl.) 106, 150–156.

He, Y., Chen, Z., Evans, A., 2008. Structural insights into aberrant topological patterns of large-scale cortical networks in Alzheimer's disease. J. Neurosci. 28, 4756–4766.

Head, D., Buckner, R.L., Shimony, J.S., Williams, L.E., Akbudak, E., Conturo, T.E., McAvoy, M., Morris, J.C., Snyder, A.Z., 2004. Differential vulnerability of anterior white matter in nondemented aging with minimal acceleration in dementia of the Alzheimer type: evidence from diffusion tensor imaging. Cereb. Cortex 14, 410–423.

Head, D., Snyder, A.Z., Girton, L.E., Morris, J.C., Buckner, R.L., 2005. Frontal-hippocampal double dissociation between normal aging and Alzheimer's disease. Cereb. Cortex 15, 732–739.

Hirono, N., Kitagaki, H., Kazui, H., Hashimoto, M., Mori, E., 2000a. Impact of white matter changes on clinical manifestation of Alzheimer's disease: a quantitative study. Stroke 31, 2182–2188.

Hirono, N., Yasuda, M., Tanimukai, S., Kitagaki, H., Mori, E., 2000b. Effect of the apolipoprotein E epsilon4 allele on white matter hyperintensities in dementia. Stroke 31, 1263–1268.

Hubbard, B.M., Anderson, J.M., 1981. A quantitative study of cerebral atrophy in old age and senile dementia. J. Neurol. Sci. 50, 135–145.

Hyman, B.T., Van Hoesen, G.W., Damasio, A.R., Barnes, C.L., 1984. Alzheimer's disease: cell-specific pathology isolates the hippocampal formation. Science 225, 1168–1170.

Jernigan, T.L., Archibald, S.L., Berhow, M.T., Sowell, E.R., Foster, D.S., Hesselink, J.R., 1991a. Cerebral structure on MRI, Part I: localization of age-related changes. Biol. Psychiatry 29, 55–67.

Jernigan, T.L., Salmon, D.P., Butters, N., Hesselink, J.R., 1991b. Cerebral structure on MRI, Part II: specific changes in Alzheimer's and Huntington's diseases. Biol. Psychiatry 29, 68–81.

Kantarci, K., Jack Jr., C.R., Xu, Y.C., Campeau, N.G., O'Brien, P.C., Smith, G.E., Ivnik, R.J., Boeve, B.F., Kokmen, E., Tangalos, E.G., Petersen, R.C., 2001. Mild cognitive impairment and Alzheimer disease: regional diffusivity of water. Radiology 219, 101–107.

Kovari, E., Gold, G., Herrmann, F.R., Canuto, A., Hof, P.R., Bouras, C., Giannakopoulos, P., 2007. Cortical microinfarcts and demyelination affect cognition in cases at high risk for dementia. Neurology 68, 927–931.

Li, S., Pu, F., Shi, F., Xie, S., Wang, Y., Jiang, T., 2008. Regional white matter decreases in Alzheimer's disease using optimized voxel-based morphometry. Acta Radiol. 49, 84–90.

Madden, D.J., Whiting, W.L., Huettel, S.A., White, L.E., MacFall, J.R., Provenzale, J.M., 2004. Diffusion tensor imaging of adult age differences in cerebral white matter: relation to response time. NeuroImage 21, 1174–1181.

Marcus, D.S., Wang, T.H., Parker, J., Csernansky, J.G., Morris, J.C., Buckner, R.L., 2007. Open Access Series of Imaging Studies (OASIS): cross-sectional MRI data in young, middle aged, nondemented, and demented older adults. J. Cogn. Neurosci. 19, 1498–1507.

Meier-Ruge, W., Ulrich, J., Bruhlmann, M., Meier, E., 1992. Age-related white matter atrophy in the human brain. Ann. N. Y. Acad. Sci. 673, 260–269.

Miller, A.K., Alston, R.L., Corsellis, J.A., 1980. Variation with age in the volumes of grey and white matter in the cerebral hemispheres of man: measurements with an image analyser. Neuropathol. Appl. Neurobiol. 6, 119–132.

Morris, J.C., 1993. The clinical dementia rating (CDR): current version and scoring rules. Neurology 43, 2412–2414.

Mungas, D., Reed, B.R., Jagust, W.J., DeCarli, C., Mack, W.J., Kramer, J.H., Weiner, M.W., Schuff, N., Chui, H.C., 2002. Volumetric MRI predicts rate of cognitive decline related to AD and cerebrovascular disease. Neurology 59, 867–873.

Mungas, D., Harvey, D., Reed, B.R., Jagust, W.J., DeCarli, C., Beckett, L., Mack, W.J., Kramer, J.H., Weiner, M.W., Schuff, N., Chui, H.C., 2005. Longitudinal volumetric MRI change and rate of cognitive decline. Neurology 65, 565–571.

Obara, K., Meyer, J.S., Mortel, K.F., Muramatsu, K., 1994. Cognitive declines correlate with decreased cortical volume and perfusion in dementia of Alzheimer type. J. Neurol. Sci. 127, 96–102.

Pfefferbaum, A., Sullivan, E.V., 2003. Increased brain white matter diffusivity in normal adult aging: relationship to anisotropy and partial voluming. Magn. Reson. Med. 49, 953–961.

Pfefferbaum, A., Mathalon, D.H., Sullivan, E.V., Rawles, J.M., Zipursky, R.B., Lim, K.O., 1994. A quantitative magnetic resonance imaging study of changes in brain morphology from infancy to late adulthood. Arch. Neurol. 51, 874–887.

Pfefferbaum, A., Sullivan, E.V., Hedehus, M., Lim, K.O., Adalsteinsson, E., Moseley, M., 2000. Age-related decline in brain white matter anisotropy measured with spatially corrected echo-planar diffusion tensor imaging. Magn. Reson. Med. 44, 259–268.

Pfefferbaum, A., Adalsteinsson, E., Sullivan, E.V., 2005. Frontal circuitry degradation marks healthy adult aging: evidence from diffusion tensor imaging. NeuroImage 26, 891–899.

Raz, N., Gunning, F.M., Head, D., Dupuis, J.H., McQuain, J., Briggs, S.D., Loken, W.J., Thornton, A.E., Acker, J.D., 1997. Selective aging of the human cerebral cortex observed in vivo: differential vulnerability of the prefrontal gray matter. Cereb. Cortex 7, 268–282.

Resnick, S.M., Goldszal, A.F., Davatzikos, C., Golski, S., Kraut, M.A., Metter, E.J., Bryan, R.N., Zonderman, A.B., 2000. One-year age changes in MRI brain volumes in older adults. Cereb. Cortex 10, 464–472.

Roher, A.E., Weiss, N., Kokjohn, T.A., Kuo, Y.M., Kalback, W., Anthony, J., Watson, D., Luehrs, D.C., Sue, L., Walker, D., Emmerling, M., Goux, W., Beach, T., 2002. Increased A beta peptides and reduced cholesterol and myelin proteins characterize white matter degeneration in Alzheimer's disease. Biochemistry 41, 11080–11090.

Rose, S.E., Chen, F., Chalk, J.B., Zelaya, F.O., Strugnell, W.E., Benson, M., Semple, J., Doddrell, D.M., 2000. Loss of connectivity in Alzheimer's disease: an evaluation of white matter tract integrity with colour coded MR diffusion tensor imaging. J. Neurol. Neurosurg. Psychiatry 69, 528–530.

Rose, S.E., McMahon, K.L., Janke, A.L., O'Dowd, B., de Zubicaray, G., Strudwick, M.W., Chalk, J.B., 2006. Diffusion indices on magnetic resonance imaging and neuropsychological performance in amnestic mild cognitive impairment. J. Neurol. Neurosurg. Psychiatry 77, 1122–1128.

Rusinek, H., de Leon, M.J., George, A.E., Stylopoulos, L.A., Chandra, R., Smith, G., Rand, T., Mourino, M., Kowalski, H., 1991. Alzheimer disease: measuring loss of cerebral gray matter with MR imaging. Radiology 178, 109–114.

Salat, D.H., Kaye, J.A., Janowsky, J.S., 1999. Prefrontal gray and white matter volumes in healthy aging and Alzheimer disease. Arch. Neurol. 56, 338–344.

Salat, D.H., Buckner, R.L., Snyder, A.Z., Greve, D.N., Desikan, R.S., Busa, E., Morris, J.C., Dale, A.M., Fischl, B., 2004. Thinning of the cerebral cortex in aging. Cereb. Cortex 14, 721–730.

Salat, D.H., Tuch, D.S., Greve, D.N., van der Kouwe, A.J., Hevelone, N.D., Zaleta, A.K., Rosen, B.R., Fischl, B., Corkin, S., Rosas, H.D., Dale, A.M., 2005a. Age-related alterations in white matter microstructure measured by diffusion tensor imaging. Neurobiol. Aging 26, 1215–1227.

Salat, D.H., Tuch, D.S., Hevelone, N.D., Fischl, B., Corkin, S., Rosas, H.D., Dale, A.M., 2005b. Age-related changes in prefrontal white matter measured by diffusion tensor imaging. Ann. N. Y. Acad. Sci. 1064, 37–49.

Salat, D.H., Tuch, D.S., van der Kouwe, A.J., Greve, D.N., Pappu, V., Lee, S.Y., Hevelone, N.D., Zaleta, A.K., Growdon, J.H., Corkin, S., Fischl, B., Rosas, H.D., 2008. White

matter pathology isolates the hippocampal formation in Alzheimer's disease. Neurobiol. Aging (2008 May 2, Electronic publication ahead of print).
Sandson, T.A., Felician, O., Edelman, R.R., Warach, S., 1999. Diffusion-weighted magnetic resonance imaging in Alzheimer's disease. Dement. Geriatr. Cogn. Disord. 10, 166–171.
Smith, C.D., Snowdon, D.A., Wang, H., Markesbery, W.R., 2000. White matter volumes and periventricular white matter hyperintensities in aging and dementia. Neurology 54, 838–842.
Stout, J.C., Jernigan, T.L., Archibald, S.L., Salmon, D.P., 1996. Association of dementia severity with cortical gray matter and abnormal white matter volumes in dementia of the Alzheimer type. Arch. Neurol. 53, 742–749.
Stoub, T.R., deToledo-Morrell, L., Stebbins, G.T., Leurgans, S., Bennett, D.A., Shah, R.C., 2006. Hippocampal disconnection contributes to memory dysfunction in individuals at risk for Alzheimer's disease. Proc. Natl. Acad. Sci. U. S. A. 103, 10041–10045.
Sullivan, E.V., Marsh, L., Mathalon, D.H., Lim, K.O., Pfefferbaum, A., 1995. Age-related decline in MRI volumes of temporal lobe gray matter but not hippocampus. Neurobiol. Aging 16, 591–606.
Sullivan, E.V., Adalsteinsson, E., Hedehus, M., Ju, C., Moseley, M., Lim, K.O., Pfefferbaum, A., 2001. Equivalent disruption of regional white matter microstructure in ageing healthy men and women. NeuroReport 12, 99–104.
Tanabe, J.L., Amend, D., Schuff, N., DiSclafani, V., Ezekiel, F., Norman, D., Fein, G., Weiner, M.W., 1997. Tissue segmentation of the brain in Alzheimer disease. AJNR Am. J. Neuroradiol. 18, 115–123.
Thal, D.R., Arendt, T., Waldmann, G., Holzer, M., Zedlick, D., Rub, U., Schober, R., 1998. Progression of neurofibrillary changes and PHF-tau in end-stage Alzheimer's disease is different from plaque and cortical microglial pathology. Neurobiol. Aging 19, 517–525.
Thomas, C., Moya, L., Avidan, G., Humphreys, K., Jung, K.J., Peterson, M.A., Behrmann, M., 2008. Reduction in white matter connectivity, revealed by diffusion tensor imaging, may account for age-related changes in face perception. J. Cogn. Neurosci. 20, 268–284.
Tohgi, H., Yonezawa, H., Takahashi, S., Sato, N., Kato, E., Kudo, M., Hatano, K., Sasaki, T., 1998. Cerebral blood flow and oxygen metabolism in senile dementia of Alzheimer's type and vascular dementia with deep white matter changes. Neuroradiology 40, 131–137.
Udaka, F., Sawada, H., Kameyama, M., 2002. White matter lesions and dementia: MRI-pathological correlation. Ann. N. Y. Acad. Sci. 977, 411–415.
van de Nes, J.A., Sandmann-Keil, D., Braak, H., 2002. Interstitial cells subjacent to the entorhinal region expressing somatostatin-28 immunoreactivity are susceptible to development of Alzheimer's disease-related cytoskeletal changes. Acta Neuropathol. (Berl.) 104, 351–356.
Vincent, J.L., Snyder, A.Z., Fox, M.D., Shannon, B.J., Andrews, J.R., Raichle, M.E., Buckner, R.L., 2006. Coherent spontaneous activity identifies a hippocampal-parietal memory network. J. Neurophysiol. 96, 3517–3531.
Wagner, A.D., Shannon, B.J., Kahn, I., Buckner, R.L., 2005. Parietal lobe contributions to episodic memory retrieval. Trends Cogn. Sci. 9, 445–453.
Wahlund, L.O., Basun, H., Almkvist, O., Andersson-Lundman, G., Julin, P., Saaf, J., 1994. White matter hyperintensities in dementia: does it matter? Magn. Reson. Imaging 12, 387–394.
Waldemar, G., Christiansen, P., Larsson, H.B., Hogh, P., Laursen, H., Lassen, N.A., Paulson, O.B., 1994. White matter magnetic resonance hyperintensities in dementia of the Alzheimer type: morphological and regional cerebral blood flow correlates. J. Neurol. Neurosurg. Psychiatry 57, 1458–1465.
Webster, B., Hansen, L., Adame, A., Crews, L., Torrance, M., Thal, L., Masliah, E., 2006. Astroglial activation of extracellular-regulated kinase in early stages of Alzheimer disease. J. Neuropathol. Exp. Neurol. 65, 142–151.
Wu, C.C., Mungas, D., Eberling, J.L., Reed, B.R., Jagust, W.J., 2002. Imaging Interactions between Alzheimer's disease and cerebrovascular disease. Ann. N. Y. Acad. Sci. 977, 403–410.
Xuereb, J.H., Brayne, C., Dufouil, C., Gertz, H., Wischik, C., Harrington, C., Mukaetova-Ladinska, E., McGee, M.A., O'Sullivan, A., O'Connor, D., Paykel, E.S., Huppert, F.A., 2000. Neuropathological findings in the very old. Results from the first 101 brains of a population-based longitudinal study of dementing disorders. Ann. N. Y. Acad. Sci. 903, 490–496.
Yang, W., Ang, L.C., Strong, M.J., 2005. Tau protein aggregation in the frontal and entorhinal cortices as a function of aging. Brain Res. Dev. Brain Res. 156, 127–138.
Zhukareva, V., Shah, K., Uryu, K., Braak, H., Del Tredici, K., Sundarraj, S., Clark, C., Trojanowski, J.Q., Lee, V.M., 2002. Biochemical analysis of tau proteins in argyrophilic grain disease, Alzheimer's disease, and Pick's disease: a comparative study. Am. J. Pathol. 161, 1135–1141.